Journal of Materials Chemistry A

Accepted Manuscript

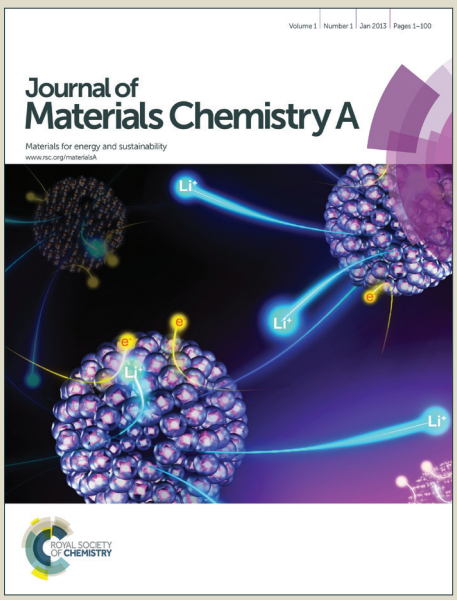

ROYAL SOCIETY OF CHEMISTRY

www.rsc.org/materialsA

Dispersion of carbon nanotubes in water by self-assembled micelles of branched amphiphilic multifunctional copolymer with photosensitivity and electroactivity

Ren Liu*, Xuebiao Zeng, Jingcheng Liu, Yuanyi Zheng, Jing Luo, Xiaoya Liu*

The Key Laboratory of Food Colloids and Biotechnology, Ministry of Education,

School of chemical and material engineering, Jiangnan University, Wuxi 214122, P.R. China

Abstract: Noncovalent surface modification has been proved to be one of the effective strategies for enhancing the properties of multi-walled carbon nanotubes (MWCNTs). When non-covalent modification method is appropriately designed, novel opportunities for better performance of CNTs can be expected. In this paper, a novel kind of branched amphiphilic photo-sensitive and electro-active copolymer (BP(VCz/VM-*alt*-MA); BPVCM) were synthesized through a simple one-pot free radical copolymerization with 7-(4-vinylbenzyloxy)-4-methyl coumarin (VM), maleic anhydride (MA), 4-vinyl benzyl thiol (VBT) and 9-(4-vinylbenzyl)-9H-carbazole (VCz) as monomers. The copolymer BPVCM can self-assemble into homogeneous spherical micelles along the side-walls of MWCNTs and efficiently disperse MWCNTs in aqueous solution. In addition, the photosensitive coumarin groups of copolymer chain undergo crosslinking under UV-irradiation, which lead to the encapsulation of MWCNTs in the crosslinked micelles and greatly improve the stability of the obtained MWCNTs suspension. More interestingly, the electroactive carbazole moieties of the BPVCM/MWCNTs composites could polymerize via electrochemical polymerization method and form a MWCNTs based conducting coating on modified glassy carbon electrode (GCE), which eventually increases electroactive sites and significantly accelerates the electron transfer. This novel preparation method permits us to obtain carbon nanotube hybrids exhibiting high water-dispersibility and stability while preserving their outstanding electrical properties, and would be valuable for construction of microelectronics and electrochemical sensors.

1 Introduction

Thanks to their outstanding physical and chemical properties, carbon nanotubes (CNTs) have promising applications in electrochemical sensors, capacitors, actuators, solar cells, etc.[1-3] However, extended van der Waals interactions between the side walls of CNTs lead to their aggregation into insoluble and unprocessable bundles of different length and diameter, which

greatly limited their practical utilities in these applications. Effective dispersing CNTs in solvents and polymer matrices remains a major challenge for both foundamental research and practical application.[4-5] So far, various carbon nanotubes dispersing techniques have been developed, which fall into two main categories: covalent functionzalization and noncovalent functionalization.[6-9] The covalent functionalization inevitably disrupts the long-range π-conjugation structure of the CNTs, resulting in partial loss of electronic properties and mechanical performance. In contrast, the noncovalent approach maintains the conjugated structure of CNTs and preserves their intrinsic properties and performance, and hence is considered more advantageous.

In a typical non-covalent modification process, the choice of organic surface-modifier is the most crucial step, thus exploring new chemical structures that can noncovalently disperse carbon nanotubes is thus of immense significance. To date, a number of non-covalent CNTs surface modifiers, including surfactants, aromatic molecules, oligomers, polymers and biomolecules, have been extensively utilized to non-covalently functionalize CNTs surface.[10-13] Among these approaches, modification of CNTs with polymeric structures has shown great promise in improving the solubility of nanotubes. The versatility of polymer chemistry allows for control over the final properties of the functionalized carbon nanotubes, which are dictated by the chemical and physical characteristics of the polymeric modifier.[14-15] The polymeric dispersing agent structurally vary from linear, star-shaped, hyperbranched, and other architectural polymers. Especially, branched and hyper-branched polymers have more advantages in dispersing CNTs because of their attractive features such as highly branched structure, multiple end groups, improved solubility, lower solution viscosity and three-dimensional globular structure.[16-19]

In recent years, amphiphilic copolymer micelle has been recognized to be a good agent to disperse CNTs in aqueous media. Kang and Taton reported the encapsulation of single-walled CNTs (SWCNTs) with the micelles formed from the amphiphilic polystyrene-*block*-poly(acrylic acid) (PS-*b*-PAA), and the resultant nano-composites are compatible with a wide variety of solvent and polymer matrices.[20] The micelles prepared from amphiphilic block copolymers, polystyrene-*block*-poly(4-vinylpyridine) (PS-*b*-P4VP), were also used to functionalize the SWCNTs through physically adhering the macromolecules to their surface, and the resulting products can be well dispersed in both polar and nonpolar solvents.[21] Engel et al. reported for SWCNTs suspensions in cross-linked PEG-terminated block copolymers (PEG-eggs), which are

stable for months.[22] Zhou reported an approach by encapsulating the CNTs into crosslinked amphiphilic hyperbranched polyester micelles.[23] Very recently, Müller demonstrated that Janus micelles were also well suited as supracolloidal dispersants for carbon nanotubes.[24]

However, in many cases, not only dissolution of CNTs but also modulation of the optoelectronic propeties of the solubilizing CNTs was desired to develop CNTs hybrid materials with novel and enhanced functional properties.[25-29] Although stable and homogenous CNTs dispersion have been achieved using amphiphilic copolymer as dispersant, the electrical property of CNTs was sacrificed due to the presence of the insulating polymer dispersant.[9,13,20,21,23] As a result, the obtained CNT/polymer nanohybrids are not so suitable for application in electronic or electrochemical devices as the insulating polymers acted as an interfacial resistor which have a detrimental effect on the electrical properties of CNTs. Hence, it is urgent to develop new amphiphilic polymers which not only disperse CNTs efficiently but also preserve the good electrical properties of CNTs.

To meet these challenges, we herein aim to develop a multifunctional polymeric dispersant that can serve as both CNTs dispersant and surface modifier simultaneously through noncovalent functionalization. In this work, we have designed and synthesized a novel branched amphiphilic multifunctional copolymer with photosensitivity and electroactivity through a simple one-pot free-radical polymerization in the presence of chain-transfer monomer and successfully applied it to non-covalently disperse MWCNTs.[30-31] Using maleic anhydride (MA), 7-(4-vinylbenzyloxy)-4-methyl coumarin (VM), vinylcarbazole (VCz) and 4-vinyl benzyl thiol (VBT) as hydrophilic, photosensitive, electroactive monomer and chain transfer monomer, respectively, the obtained copolymer (BP(VCz/VM-*alt*-MA); BPVCM) consist of hyperbranched architecture with a number of hydrophilic anhydride groups and hydrophobic coumarin and carbazole groups (Scheme 1). This amphiphilic branched copolymer can form micelles in water which physically adheres to the surface of MWCNTs and efficiently disperse MWCNTs in aqueous solution. Such a unique molecular structure and composition make BPVCM very suitable to non-covalently modify MWCNTs surfaces owing to the following reason: First, compared to most water-based dispersants, BPVCM can disperse a large amount of MWCNTs with good dispersing quality, possibly owing to the branched structure of BPVCM. Second, the photosensitive coumarin groups of copolymer chain undergo crosslinking under UV-irradiation,

which lead to the encapsulation of MWCNTs in the crosslinked micelles and greatly improve the stability of the obtained MWCNTs suspension. Third, the carbazole units in copolymer chains could electro-polymerize with electrochemical method, thus creating large conjugated system and forming a conducting composite, which eventually enhanced the conductivity and significantly accelerate the electron transfer of the resulted BPVCM/MWCNTs hybrid film.

2 Experimental

2.1 Experimental Materials

The photosensitive monomer 7-(4-vinylbenzyloxy)-4-methyl coumarin (VM) was synthesised from 4-vinylbenzyl chloride (Acros Organics) and 7-hydroxy-4-methylcoumarin (Acros Organics) according to the literature protocol.[32] 2, 2′-azobis (isobutyronitrile) (AIBN) and maleic anhydride (AnalaR, Aladdin) (MA) were recrystallized twice from acetone before use. Carbazol and 4-vinylbenzyl chloride were provided by J&K Chemical Co. Ltd. Tetramethylene oxide (THF), N, N-dimethylformamide (DMF) and toluene (Shanghai Chemical Reagent Co., Ltd.) were of analytical grade and used as received without further purification. Chain transfer monomer, 4-vinyl benzyl thiol (VBT), was synthesized from 4-vinylbenzyl chloride and thiourea according to the literature protocol.[33] MWCNTs (>95%) were provided by Chengdu Organic Chemicals Institute, Chinese Academy of Sciences, China. All solvents and other reagents were purchased from Shanghai First Reagent Co., China.

2.2 Measurements

The ^{1}H NMR spectra were recorded with a Bruker DMX500 MHz spectrometer. The molecular weight and molecular weight distribution index of the copolymers were determined using gel permeation chromatography (GPC, HP1100) with THF as amobile phase at a flow rate of 1.0 mL/min at 35 °C. Polystyrene standards were used for the calibration of the molecular weight. Molecular weight and macromolecular structure parameters of samples in THF were measured by size exclusion chromatography/multiangle laser light scattering (SEC/MALLS) equipment coupled with viscometer (Viscostar, Wyatt Technology). The THF elution velocity was set as 1.0 mL/min. The chromatography system consisted of gel columns (Waters Styragel), an autosampler and a differential refractometer (Optilab rEX). The refractive index increment (dn/dc) value of polymer in THF solution was determined by a refractive index detector (Optilab rEX, Wyatt

Technology) at 25 °C. UV-vis absorption spectra were taken on a HP8452 spectrophotometer. The photodimerization degree (PD) was calculated from the UV-vis spectra by comparing the peak absorption at 320 nm assigned to the coumarin group by the following equation: PD % = $(A_0-A_t)/A_0$. Here, A_0 and A_t are the peak absorptions centered at 320 nm assigned to the coumarin group. 0 and t represent before irradiation and after the t time of irradiation by light. Raman spectra were recorded using a Renishaw equipped with a charge-coupled device detector at 785 nm laser. Fluorescence spectra were recorded with a Shimadzu RF-5301PC spectrometer by excitation at 352 nm (excitation slit width: 5 nm; emission slit width: 5 nm) at 25 °C. High-resolution transmission electron microscopy (HR-TEM) images were obtained on a JEOL-2010 transmission electron microscope. A Hitachi S-4800 scanning electron microscope (produced in Japan) was used to observe the surface morphologies of the samples. A conventional three-electrode system was employed, involving a modified glassy carbon disk electrode (GCE) as the working electrode, a platinum wire as the counter electrode and a saturated calomel electrode (SCE) as the reference electrode.

2.3 Synthesis and characterizations of VCz

The detail synthesis route and characterizations of VCz were described in the supporting information and the ^{1}H NMR spectrum of VCz was shown in Fig. S2.

2.4 Synthesis and characterizations of BP(VCz/VM-alt-MA)

Scheme 1

BPVCM was synthesized through a free-radical copolymerization. VBT, VM, MA,VCz were dissolved in dioxane at different molar ratios in a round-bottom flask and AIBN was then added. After stirring at room temperature for 30 minutes, the mixture was placed in a preheated oil bath (65 °C) for 24 h with stirring. The resultant copolymers were purified by reprecipitation three times from toluene and then dried under vacuum at room temperature for 24 h. As a control experiment, linear copolymers P(VCz/VM-*alt*-MA) (LPVCM) were prepared under identical conditions to those used in preparing BPVCM but in the absence of VBT. Table S1 shows the designation of linear and branched polymer BPVCM with different polymerization times and different content of VBT. The subscript of the sample ($BPVCM_{t2\text{-}t24}$) is the different

polymerization time and that of ($BPVCM_{4-16}$) is the different content of VBT.

2.5 Preparation of BPVCM functionalized MWCNTs aqueous dispersion

Pristine MWCNTs (0.8-12 mg) was added into 1 mL of DMF solution containing 2-10 mg of BPVCM copolymer with the aid of sonication for 1 h. Then, 2 mL of deionised water was added dropwise at 0.1 mL/min to induce the formation of micelles around the nanotubes.

After magnetic stirring for 1 h, additional deionised water was added dropwise to the mixture at a rate of 0.1 mL/min until the DMF/H_2O ratio reached 1 : 9 (wt %) before they were dialyzed against water to remove the remaining DMF. The copolymer underwent partial hydrolysis in water during this process and produced a large amount of carboxyl groups that made the modified nanotube negatively charged in neutral solution. The homogeneous nanocomposite was cross-linked by irradiation with UV light (without the cross-linker and the initiator, $\lambda > 310$ nm). Finally, the resultant suspension was filtered through a short plug of glass wool to remove the undispersed materials, which yielded BPVCM micelle functionalized MWCNTs aqueous dispersion (Scheme 2).

Scheme 2

2.6 Determination of the MWCNTs solubility

12 mg MWCNTs and 2 mg $BPVCM_4$ were mixed with 1 mL DMF in a glass vial, followed by bath sonication in water/ice at 0 °C for 1 h, deionised water was added dropwise to the sonicating mixture until the DMF/H_2O ratio reached 1 : 9 (wt %) at a rate of 0.1 mL/min, the dispersion were dialyzed to remove DMF. The resulting dispersion was shaken at 400 rpm for 24 h at room temperature. Then the solution with suspended MWCNTs was carefully decanted and saved, and the unsolubilized MWCNTs precipitated at the bottom of the glass vial were dried in a vacuum oven at 100 °C for 5 h and then weighed to determine the mass of the unsolubilized MWCNTs. Subtracting this mass from the original mass of MWCNTs gave the mass of solubilized MWCNTs.

2.7 Fabrication of BPVCM/MWCNTs modified glassy-carbon electrode

GCE (3 mm in diameter) was used to fabricate the modified electrode. GCE was first polished on finer sandpaper, further followed by alumina slurry (0.3 μm and 0.05 μm particles) on polishing pad, with intermediate 10 min sonication in water between each polishing step. A 5 μL

$BPVCM_4$ functionalized MWCNTs aqueous dispersion (1 : 4 wt%, 0.8 mg/mL of MWCNTs aqueous solution) was uniformly cast onto the pretreated bare GCE surface and dried at room temperature for at least 24 h.

The obtained BPVCM/MWCNTs film was then electrochemically cross-linked using CV. CV experiments were carried out on a Epsilon electrochemical workstation (BAS, USA) using a three-electrode setup from a solution of 0.1 M $LiClO_4$ dissolved in acetonitrile (ACN). The BPVCM/MWCNTs film modified GCE was used as the working electrode (WE), a platinum wire as the counter electrode (CE), and a saturated calomel electrode (SCE) as the reference electrode (RE). Electrochemical cross-linking of BPVCM and MWCNTs nanocomposite film was accomplished by repeatedly cycling the electrode potential between the potential range of 0 to 1.5 V for up to 20 cycles at a potential scan rate of 100 mV/s. The highly cross-linked nanocomposite film was thoroughly washed with deionised water and was dried in nitrogen before its analysis.

Electrochemical impedance spectroscopy (EIS) (CHI 660C electrochemical analyzer, Chenhua Corp., Shanghai, China) was used to investigate the impedance properties of the BPVCM/MWCNTs nanocomposite and cross-linked films. EIS measurements were performed under an open circuit potential in an AC frequency range from 100 000 to 0.01 Hz with an excitation signal of 5 mV. All electrochemical experiments were carried out at room temperature.

3 Results and discussion

3.1 Synthesis of the BPVCM copolymer

The amphiphilic hyperbranched copolymer used here was conveniently synthesized through a facile one-pot free radical polymerization in the presence of chain transfer agent using maleic anhydride (MA), 7-(4-vinylbenzyloxy)-4-methyl coumarin (VM) and vinylcarbazole (VCz) as hydrophilic, photosensitive and electroactive monomer, respectively. Scheme 1 shows the synthetic route of the amphiphilic hyperbranched copolymer BPVCM. Recently, our group and Jiang's group reported the synthesis of branched vinyl polymer through radical polymerization in the presence of chain transfer monomer which contains a polymerizable vinyl group and a chain transferring/initiating thiol group.[30,31,33,35] The vinyl group of chain transfer monomer participated in the polymerization and the thiol group formed a sulfur radical which initiated the chain transfer/intiating reaction, generating the branched macromolecules.

Fig. S3 shows the ^{1}H NMR spectrum of the obtained copolymer BPVCM. As shown in Fig. S3, the signals at 6.4-7.9 ppm (H13, H14, H21, H24-26, H28 and H29) are assigned to the aromatic protons of carbazole and courmarin groups. The peaks at 1.0 (H1, H5, H9) and 2.0 (H19) ppm are ascribed, respectively, to the methyl protons and the methylene protons in the polymer unit. The signal at 6.1-6.4 ppm (H20) corresponds to the protons of VM. The signals at 3.6 and 2.6 ppm (H11, H12) were assigned to the protons of the MA group. Consequently, the structures of the copolymers BPVCM can be confirmed through ^{1}H NMR results.

Fig. 1

To investigate the branched polymerization, six branched polymers of $BPVCM_{t2\text{-}t24}$ with different polymerzing time were designed as listed in Table S1 and prepared via one-pot synthesis at 65 °C. For comparison, linear polymer (LPVCM) was also prepared under the same experimental condition only without the addition of the chain transfer monomer. The $BPVCM_{t2\text{-}t24}$ copolymers with various polymerization times were characterized by triple detection system, and the details are given in Table S2. The conversion of the branched polymers increases with the polymerization time. It is obvious that the molecular weights of branched polymers increased with increasing polymerization time. And the effect of architectural branching can also be expressed by the Zimm branching factor g', which is defined as $g' = [\eta]_b/[\eta]_l$, where $[\eta]_b$ and $[\eta]_l$ are the obtained intrinsic viscosity of branched and linear polymers in solvent.[31,37] The magnitude of g' decreased linearly along with the polymerization time and the branched polymer $BPVCM_{t24}$ gained the lowest g' value of 52%, which indicates that much more VBT monomers were copolymerized into the polymer chains to form branches along with the polymerization time.

It is known that MarkHouwink shape parameter ($[\eta] = KM^{\alpha}$) of the branched polymers has lower values than those of their linear counterparts.[36] Fig. 1A shows the classical MarkHouwink plot of $BPVCM_{t24}$ and corresponding linear polymer (LPVCM). It is clearly observed that the intrinsic viscosity ([η]) of branched copolymer is lower than that of linear polymer. In addition, the slope of the intrinsic viscosity versus M_w is much lower than that of linear counterpart (α = 0.844 for linear polymer versus 0.472 for branched polymer), which is consistent with the compact and globular shape of branched polymer compared to their linear counterpart.[36-37] The

decrease of the glass-transition temperature (T_g) and g' on the varied polymerization time in Fig. 1B also demonstrates this branch growth.[33] With increasing polymerization time, the curve of T_g and g' of $BPVCM_{t2\text{-}t24}$ showed a decline trend and then reached a flat area. The possible reason is that the chain transfer polymerization occurred at the early stage of polymerization and the increasing degree of branching of BPVCM resulted in less entanglement between the polymer chains, which facilitates the movement of the BPVCM polymer chains and leads to the decrease in the T_g of BPVCM.[35] The above results clearly demonstrated the successful preparation of BPVCM.

Fig. 2

The BPVCM copolymer was an amphiphilic macromolecule and thus could self-assemble into micelle in selective solvent. The MA units of the copolymer easily hydrolyzed into carboxyl group and thus functioned as hydrophilic component, and VM, VCz units functioned not only as photosensitive and electroactive monomer but also as hydrophobic components. The prepared BPVCM was confirmed to form micelles by TEM and the morphology of the self-assembled micelles was shown in Fig. 2. It is clearly observed that the self-assembled micelles of all copolymers are spherical and in the size range of 80-150 nm. The variation in preparation condition (different content of the transfer monomer VBT) of the copolymer does not have great impact on the size and shape of the self-assembled micelles. In contrast, the concentration of the copolymer significantly influenced the size of the obtained micelles. As shown in Fig. S5. the micelle diameter increased from 80 nm to 350 nm with the increasing concentration of the copolymer from 0.2 to 1.0 mg/mL.

3.2 Dispersion of MWCNTs with BP(VCz/VM-alt-MA)

Fig. 3

0.8 mg MWCNTs was added into 1 mL of DMF solution containing 2 mg of LPVCM or BPVCM copolymer with the aid of sonication for 1 h. Deionised water was added dropwise to the

mixture to induce the formation of micelles around the nanotubes until the DMF/H_2O ratio reached 1 : 9 (wt %) before they were dialyzed against water to remove the remaining DMF. The dispersion efficiency of MWCNTs in aqueous solution without polymers or with polymers were observed by visual observation as shown in Fig. 3. The pristine MWCNTs dispersion began to precipitate immediately after sonication and completely settled at the bottom of vial within 0.5 h (Fig. 3A). In contrast, copolymers functionalized MWCNTs exhibited black-coloured ink-like dispersion and no precipitation were observed after thirty days of standing (Fig. 3B, C, D, E, F). The good dispersibility of the functionalized MWCNTs allowed UV-vis absorption spectra to be recorded. Fig. S6 presents the UV-vis absorption spectra of BPVCM functionalized MWCNTs aqueous dispersions with different concentrations. These curves were similar and featureless, similar to reported functionalized MWCNTs with other polymer dispersant.[47] The absorption intensity increases with the increasing concentration of MWCNTs dispersion. The dependence of absorbance intensity at 500 nm obeys Beer's law (the inset of Fig. S6) and was linearly dependant on the concentration of the samples, indicating that the dispersion of functionalized MWCNTs in water was homogeneous and there was no optical behavior typically caused by the aggregation of MWCNTs. Moreover, the MWCNTs loadings obtained by using $BPVCM_4$ as the dispersant can reach as high as 0.8 mg/mL, which exceed most of the reported values for CNTs dispersions in aqueous solutions using other non-covalent type dispersant (Fig. 3). This is quite important for producing high concentration of MWCNTs dispersion for the fabrication of MWCNTs based sensing, switcher and optical limiter.

Fig. 4

To investigate the influence of the preparation condition of the copolymer on the dispersion efficiency of MWCNTs, the dispersion state and its long-term stability of MWCNTs functionalized by different copolymer was examined more quantitatively by UV-vis spectroscopy. The absorbance values were recorded at the wavelength of 500 nm as reported in previous studies[48] (wavelength of 500 nm was chosen as this wavelength is virtually unaffected by ambient conditions of nanotubes) and is plotted against time of still-standing for dispersion samples, as shown in Fig. 4. According to the Beer-Lambert's law, the dissolved amount of nanotubes is

linearly proportional to the UV absorbance, thus a higher UV-vis absorbance means a larger aqueous dispersibility of the functionalized carbon nanotube. For MWCNTs functionalized with linear polymer, the absorbance decreases to 72% of its initial value over a period of one month. For branched copolymer functionalized MWCNTs, the absorbance also decreases with the time, but the decreased extent is less than that of linear counterpart. Especially for $BPVCM_4$ functionized MWCNTs, the absorbance preserved 83% of its initial value after 30 days. This result indicates that branched structure is beneficial in improving the dispersion stability of MWCNTs in aqueous solution.

Fig. 5

The morphology of pristine MWCNTs and MWCNTs with different polymers was characterized by TEM. It was observed that the pristine MWCNTs are densely entangled caused by the large van der Waals forces and its surface is quite smooth as shown in Fig. 5. In contrast, well-separated nanotubes are observed for BPVCM functionalized MWCNTs, showing that MWCNTs was effectively dispersed by branched copolymer. In addition, the existence of a layer of copolymer micelles attaching on the surface of carbon nanotubes are apparent, indicating effective functionalization of MWCNTs by branched copolymer micelles. This observation demonstrates that the strong adsorption of BPVCM micelles onto the surface of MWCNTs results in breaking up the interaction between MWCNTs in coagulated CNTs bundles, which suppresses reaggregation of the MWCNTs and promotes the formation of a stable dispersion. Similar observation that micelles adsorbed on the surface of carbon nanotubes has been reported by Park[21] and Müller[24], who employed PS-*b*-P4VP20 block copolymer micelles and Janus polymer micelles to disperse CNTs, respectively. It should be noted that preparation condition (different content of the transfer monomer VBT) of the copolymer has not much effect on the morphology of copolymer functionalized MWCNTs. We also examined the effect of the copolymer concentration on the morphology. It is observed that with the increasing concentration of the branched copolymer $BPVCM_4$, the diameter of the micelles adhering to the surface of MWCNTs increased accordingly. And when the concentration of $BPVCM_4$ reaches 1.0 mg/mL, a large number of free

copolymer micelles is clearly observed, which is possibly attributed to the assembly of the excess copolymer with each other instead of attaching to MWCNTs. The SEM images showed the same trend (Fig. 6).

Fig. 6

Previous literatures provided many dispersing mechanism for MWCNTs in solution using amphiphilic polymer micelles. Islam proposed that SWCNTs were stabilized by hemimicelles of sodium dodecylbenzene sulfonate surfactant due to stiffness of the surfactant as well as π-liking stacking of the benzene rings onto surface of SWCNTs.[49] Park attributed the dispersion of SWCNTs to the physical adsorption of micelles onto surface of SWCNTs.[21] The recent study by Müller who used Janus micelle as dispersant showed that Janus micelle adsorb to the MWCNTs with a π-liking stacking hemisphere, while stabilizing the supracolloidal hybrid in the chosen medium through steric repulsion with a solvophilic hemisphere and also demonstrated that the Janus balance (the size ratio of both corona patches show critical impact on the effectiveness of the dispersant).[24] Based on the above literatures and the TEM images, the dispersing mechanism of BPVCM for MWCNTs in our study may be explained as follows: In our system, initially, the BPVCM copolymer and MWCNTs were co-dissovled in DMF by sonication. Owing to strong π-π interaction between MWCNTs and the aromatic moieties along the polymer chain, the BPVCM chain are strongly attached to the surfaces of MWCNTs. With the addition of water, the BPVCM self-assemble into uniform spherical micelles along the surface of the MWCNTs, stabilizing the MWCNTs in aqueous solution through steric repulsion with a solvophilic hemisphere (Fig. $6B_{1,2}$). With the increasing concentration of BPVCM, the micelle diameter increases (Fig. S5), which enhance surface-energy of micelles and lead to the repulsion and disjoining between BPVCM micelles on the surface of MWCNTs (Fig. $6C_{1,2}$). With the further increasing BPVCM concentration, the excessive BPVCM can self-assemble not only along the side-walls of the nanotubes but also in the water (Fig. $6D_{1,2}$), inducing aggregation of micelles and undermine the stability of the MWCNTs suspension.

3.3 The interaction between BPVCM and MWCNTs

The nature of interaction between BPVCM micelles and MWCNTs was investigated by

Raman spectroscopies with an excitation wavelength at 785 nm. Fig. S7A shows the Raman spectra of pristine MWCNTs and BPVCM functionalized MWCNTs. The pristine MWCNTs show a D-band at 1317cm^{-1} and a G-band at 1614 cm^{-1}. For the MWCNTs functionalized with BPVCM, the D- and G-bands are blue-shifted to 1306 and 1599 cm^{-1}. The blueshift between pristine and polymer functionalized MWCNTs has been reported in many previous literatures which was attributed to charge-transfer and π-π stacking interactions between the polymer and MWCNTs.[19,59] In our system, it is quite possible that there is charge transfer between the BPVCM polymer and the MWCNTs considering that carbon nanotubes easily accept electron and carbazole groups in BPVCM polymer easily donate electron, which increases the energy necessary for vibrations and shifts the Raman band to the higher frequency.[60-61]

The strong π-π interaction between copolymer and the carbon nanotubes is further evidenced by the fluorescence spectroscopy. MWCNTs are metalic and have been observed to be a highly effective quencher for the conjugated polymer fluorescence owing to the intermolecular electronic energy transfer and charge transfer between MWCNTs and aromatic polymers.[50-51] Owing to the presence of aromatic coumarin and carbazole groups in the polymer chain, $BPVCM_4$ shows strong fluorescence at 445 nm. For $BPVCM_4$ functionalized MWCNTs, MWCNTs are expected to efficiently quench the fluorescence of $BPVCM_4$ if the π electrons of coumarin and carbazole groups interact with the π conjugated CNT surfaces. As is shown in Fig. S7B, BPVCM functionalized MWCNTs exhibits similar emission band, while the intensity is significantly reduced relative to that of free $BPVCM_4$, indicating that the quenching takes place between $BPVCM_4$ and the MWCNTs surface in BPVCM/MWCNTs solution. Note that the concentration of $BPVCM_4$ in both samples remained constant (0.2 mg/mL). The shift in the emission peak and this remarkable fluorescence quenching strongly for the BPVCM/MWCNTs relative to the $BPVCM_4$ may be attributed to the strong π-π interactions between coumarin and carbazole rings of $BPVCM_4$ and the MWCNTs.

3.4 Photosensitivity of BPVCM modified MWCNTs

Fig. 7

It is well-known that the direct irradiation (λ > 300 nm) of coumarin leads to photochemical

dimerization, resulting in cyclobutane-type dimmers.[52-53] The presence of coumarin units on the copolymer chains endows the $BPVCM_4$ micelle photosensitivity. Fig. 7 shows UV-vis spectroscopy of $BPVCM_4$ micelle aqueous solution at different irradiation time. When the solution of copolymer micelle is exposed to UV light of 365 nm (400 mW from a spot LED curing system), the absorbance at around 320 nm characteristic of coumarin group decreased continuously with prolonging the irradiation time, indicating the dimerization of neighboring coumarin moieties. As the coumarin dimerizes, the level of unsaturation decreases due to the formation of crosslinking. Therefore, the decrease in the absorption intensity at 320 nm can be primarily attributed to the loss of the coumarin chromophores resulting from the UV light-induced photodimerization. The inset of Fig. 7 depicts the dependence of the dimerization degree of coumarin in the micelles on UV irradiation time. It can be observed that the dimerization degree abruptly increased during the first 15 mins' photoirradiation and reached a platform, indicating that the saturation point has reached. The estimated maximum photodimerization degree based on the absorbance change at 320 nm in the inset is about 60%, indicating most of coumarin group has been photocrosslinked.

Fig. 8

Several papers reported that encapsulating carbon nanotubes within crosslinked, amphiphilic copolymer micelle was beneficial for preparing stable CNTs dispersions.[23,54,55] We expect to see that after the photocrosslinking of the copolymer micelles upon photoirradiation, the MWCNTs can be encapsulated in the photocrosslinked micelles, and a more stable aqueous dispersion of MWCNTs should be obtained. To evidence this assumption, the absorbance values of BPVCM functionalized MWCNTs after photoirradiation at 500 nm is plotted against time of still-standing for dispersion samples, as shown in Fig. 8. The absorbance of sample without irradiation drops down to 79% of its initial value after 1 month. In contrast, for the sample after photoirradiating, the absorbance intensity decayed much slower and maintained 90% of its initial value over a period of 1 month, which suggests that the stability of the MWCNTs dispersion becomes better by the photoirradiation. In addition, a large quantity of black MWCNTs precipitate was observed at the bottom of the glass vial for the MWCNTs dispersion without photoirradiation, whereas the sample after photoirradiation exhibit only little black MWCNTs precipitate (as shown in the inset

of Fig. 8), which vividly confirmed the improved stability. The enhanced stability of BPVCM functionalized MWCNTs aqueous dispersion after irradiation with UV light could be explained as following: owing to the presence of photosensitive coumarin groups in the BPVCM micelles along the surface of the MWCNTs, the UV irradiation leads to the photo-crosslinking of micellar shells around the MWCNTs which could encapsulate carbon nanotubes in $BPVCM_4$ micells (as shown in Scheme 2) and stabilize the noncovalent functionalization.[20,22,23]

3.5 Electrochemical crosslinking of BPVCM/MWCNTs

Fig. 9

Carbazole is one of the electro-active units which could electro-polymerize to form large conjugate structure named polycarbazole (PCz).[56] Assuming that the carbazole moiety on the side chain of $BPVCM_4$ copolymer was attached on the surface of MWCNTs, the electropolymerization of carbazole could create a π-conjugated conductive network containing both inter- and intramolecular cross-linkages between the pendant carbazole units (the inset of Fig. 9) on the surface of MWCNTs and thus enhance the electrical properties of BPVCM/MWCNTs. The electrochemical cross-linking of the carbazole moieties was executed by employing CV and Fig. 9 shows the first 20 cycles of the CV traces of BPVCM/MWCNTs films with a potential scale from 0 to 1.5 V at a scan rate of 100 mV/s in 0.1 M $LiClO_4$/ACN. The oxidation onset at about 1.1~1.2 V in the first cycle results from the formation of the carbazolylium radical cations which allowed subsequent start of electropolymerization of the carbazole units via 3,6 connectivity in the films.

Fig. 10

Electrochemical impedance spectroscopy (EIS) is a well-known and powerful tool for determing interfacial charge-transfer of films.[57-58] To evaluate the effect of carbazole electropolymerization on the interfacial properties of BPVCM/MWCNTs, the impedance spectra of BPVCM/MWCNTs before and after electropolymerization were recorded and shown in Fig. 10A. The Nyquist disgram of bare GC electrode was also provided for comparison. Obviously, all Nyquist diagrams include a semicircle region at higher frequencies, followed by a straight line at

lower frequencies for the three electrodes. The semicircular region corresponds to the electron transfer limited process, and the diameter is equivalent to the electron transfer resistance (Rct) which normally reflects the conductivity and the electron transfer process. As for the linear portion, it corresponds to the diffusion-controlled electrochemical process of $[Fe(CN)_6]^{3-/4-}$ at the electrode surface. As shown in Fig. 10A, BPVCM/MWCNTs modified GCE exhibits a semicircle with diameter of 1.54 (Z'/KΩ), much larger than that of bare GC electrode, indicating BPVCM/MWCNTs has a larger electron transfer resistance than bare GCE. After electropolymerization of carbazole, the semicircle was reduced obviously with comparison of that for sample before electropolymerization and even smaller than that of bare GCE, implying that electropolymerization significantly accelerating the transfer of the electrons. The current change of $[Fe(CN)_6]^{3-/4-}$ on the three electrodes recorded by CV method also confirmed the same result, as shown in Fig. 10B. The peak current of the BPVCM/MWCNTs after electropolymerization (blue curve in Fig. 10B) was much larger than that of the sample before electropolymerization (red curve in Fig. 10B). In addition, the potential separation of the redox peak also became narrowed after electropolymerization. The above results demonstrate that the electro-polymerization of carbazole enhanced the current response and accelerates the electron transfer of BPVCM/MWCNTs hybrid, which creates CNT-functionalized surfaces with many potential applications such as nanotube-based sensing and electrocatalysis.

4 Conclusions

We have demonstrated a simple and novel strategy to disperse and stabilize MWCNTs in water using self-assembling micelles of a novel photo-sensitive and electroactive amphiphilic branched copolymer BPVCM. TEM images showed a dense coating of micelle on the surface of MWCNTs, which hindered the aggregation of carbon nanotubes. The BPVCM micelles not only serve as dispersant and stabilizer, but also as surface modifier. The photosensitive coumarin groups in BPVCM chain undergo crosslinking under UV-irradiation and result in encapsulation of MWCNTs in the crosslinked micelles, which greatly improve the stability of the obtained MWCNTs suspension. Furthermore, the electroactive carbazole units of the BPVCM/MWCNTs composites could polymerize via electrochemical method and forming a conducting coating modified glassy carbon electrode (GCE), which eventually increases electroactive sites of the

modified GCE and significantly accelerates the electron transfer. This noncovalent modification of MWCNTs with multifunctional polymer micelles will have a promising application in high performance microelectronics and electrochemical sensors.

Acknowledgments

We acknowledge financial support from the National Natural Science Foundation of China (No. 51103064), the Fundamental Research Funds for the Central Universities (JUSRP 51305A). We thank Prof. Daoyong Chen for helping in the discussion of dispersing mechanism of BPVCM for MWCNTs.

References

1 M. A. McCarthy, B. Liu, E. P. Donoghue, I. Kravchenko, D. Y. Kim, F. So and A. G. Rinzler, *Science*, 2011, 332, 570-573.

2 J. Wang, R. P. Deo, P. Poulin and M. Mangey, *J. Am. Chem. Soc*., 2003, 125, 14706-14707.

3 M. F. L. De Volder, S. H. Tawfick, R. H. Baughman and A. J. Hart, *Science*, 2013, 339, 535-539.

4 L. Hu, D. S. Hecht and G. Grüner, *Chem. Rev.,* 2010, 110, 5790-5844.

5 E. Nativ-Roth, R. Shvartzman-Cohen, C. Bounioux, M. Florent, D. Zhang, I. Szleifer and R. Yerushalmi-Rozen, *Macromolecules*, 2007, 40, 3676-3685.

6 N. G. Sahoo, S. Rana, J. W. Cho, L. Li and S. H. Chan, *Prog. Polym. Sci*., 2010, 35, 837-867.

7 N. Roy, R. Sengupta and A. K. Bhowmick, *Prog. Polym. Sci*., 2012, 37, 781-819.

8 N. Karousis, N. Tagmatarchis and D. Tasis, *Chem. Rev*., 2010, 110, 5366-5397.

9 A. Prevoteau, C. Soulié-Ziakovic and L. Leibler, *J. Am. Chem. Soc*., 2012, 134, 19961-19964.

10 K. K. Kim, S. M. Yoon, J. Y. Choi, J. Lee, B. K. Kim, J. M. Kim, J. H. Lee, U. Paik, M. H.

Park, C. W. Yang, K. H. An, Y. Chung and Y. H. Lee, *Adv. Funct. Mater*., 2007, 17, 1775-1783.

11 J. Zou, L. Liu, H. Chen, S. I. Khondaker, R. D. McCullough, Q. Huo and L. Zhai, *Adv Mater*., 2008, 20, 2055-2060.

12 V. Datsyuk, P. Landois, J. Fitremann, A. Peigney, A. M. Galibert, B. Soula and E. Flahaut, *J. Mater. Chem*., 2009, 19, 2729-2736.

13 R. Haggenmueller, S. S. Rahatekar, J. A. Fagan, J. Chun, M. L. Becker, R. R. Naik, T. Krauss, L. Carlson, J. F. Kadla, P. C. Trulove, D. F. Fox, H. Delong, Z. Fang, S. O. Kelley and J. W. Gilman, *Langmuir,* 2008, 24, 5070-5078.

14 A. T. Chien, P. V. Gulgunje, H. G. Chae, A. S. Joshi, J. Moon, B. Feng, G. P. Peterson and S. K. Kumar, *Polymer*, 2013, 54, 6210-6217.

15 X. Q. Liu, Y. L. Li, Y. W. Lin, S. Yang, X. F. Guo, Y. Li, J. Yang and E. Q. Chen, *Macromolecules*, 2013, 46, 8479-8487.

16 A. Star and J. F. Stoddart, *Macromolecules*, 2002, 35, 7516-7520.

17 K. Petrie, A. Docoslis, S. Vasic, M. Kontopoulou, S. Morgan and Z. Ye, *Carbon*, 2011, 49, 3378-3382.

18 G. Yu, M. Xue, Z. Zhang, J. Li, C. Han and F. Huang, *J. Am. Chem. Soc*., 2012, 134, 13248-13251.

19 H. Li and J. J. Cooper-White, *Nanoscale*, 2013, 5, 2915-2920.

20 Y. Kang and T. A. Taton, *J. Am. Chem. Soc*., 2003, 125, 5650-5651.

21 H. I. Shin, B. G. Min, W. Jeong and C. Park, *Macromol. Rapid Commun*., 2005, 26, 1451-1457.

22 R. Wang, P. Cherukuri, J. G. Duque, T. K. Leeuw, M. K. Lackey, C. H. Moran, V. C. Moore, J. L. Conyers, R. E. Smalley, H. K. Schmidt, R. B. Weisman and P. S. Engel, *Carbon*, 2007, 45, 2388-2393.

23 W. Zhou, S. Lv and W. Shi, *European Polymer Journal*, 2008, 44, 587-601.

24 A. H. Gröschel, T. I. Löbling, P. D. Petrov, M. Müllner, C. Kuttner, F. Wieberger and A. H. Müller, *Angew. Chem. Int. Ed.*, 2013, 52, 3602-3606.

25 H. Acharya, J. Sung, H. I. Shin, S. Y. Park, B. G. Min and C. Park, *React. Funct. Polym.*, 2009, 69, 552-557.

26 Y. Wei, L. T. Kong, R. Yang, L. Wang, J. H. Liu and X. J. Huang, *Chem. Commun.*, 2011, 47, 5340-5342.

27 P. D. Petrov, G. L. Georgiev and A. H. Müller, *Polymer*, 2012, 53, 5502-5506.

28 G. Clavé, G. Delport, C. Roquelet, J. S. Lauret, E. Deleporte, F. Vialla, B. Langlois, R. Parret, C. Voisin, P. Roussignaol, B. Jousselme, A. Gloter, O. Stephan, A. Filoramo, V. Derycke and S. Campidelli, *Chem. Mater.,* 2013, 25, 2700-2707.

29 W. Wenseleers, I. I. Vlasov, E. Goovaerts, E. D. Obraztsova, A. S. Lobach and A. Bouwen, *Adv. Funct. Mater.*, 2004, 14, 1105-1112.

30 J. Liu, Y. Wang, Q. Fu, X. Zhu and W. Shi, *J. Polym. Sci., Part A: Polym. Chem.*, 2008, 46, 1449-1459.

31 L. Jiang, W. Huang, X. Xue, H. Yang, B. Jiang, D. Zhang, J. Fang, J. Chen, Y. Yang, L. Kong and S. Wang, *Macromolecules*, 2012, 45, 4092-4100.

32 X. Liu, C. Yi, Y. Zhu, Y. Yang, J. Jiang, Z. Cui and M. Jiang, *Journal of Colloid and Interface Science,* 2010, 351, 315-322.

33 J. Liu, X. Xiong, R. Liu, J. Jiang and X. Liu, *Polym. Bull*., 2013, 70, 1795-1803.

34 Y. Liu, N. Li, X. Xia, Q. Xu, J. Ge and J. Lu, *Materials Chemistry and Physics*, 2010, 123, 685-689.

35 J. Jiang, X. Jia, X. Chen, Y. Zong, H. Zhang, L. Lin, X. Liu and M. Chen, *Chem. Lett*., 2011, 40, 1378-1380.

36 J. M. Fréchet, M. Henmi, I. Gitsov, S. Aoshima, M. R. Leduc and R. B. Grubb, *Scienc*e, 1995, 269, 1080-1083.

37 H. J. Yang, B. B. Jiang, W. Y. Huang, D. L. Zhang, L. Z. Kong, J. H. Chen, C. L. Liu, F. H. Gong, Q. Yu and Y. Yang, *Macromolecules*, 2009, 42, 5976-5982.

38 T. Liu, G. Xu, J. Zhang, H. Zhang and J. Pang, *Colloid Polym Sci.*, 2013, 291, 691-698.

39 H. Gao, S. Zhang, D. Huang and L. Zheng, *Colloid Polym Sci*., 2012, 290, 757-762.

40 M. G. Adsul, D. A. Rey and D. V. Gokhale, *J. Mater. Chem*., 2011, 21, 2054-2056.

41 W. Zhang and S. R. P. Silva, *Spectrochim Acta Part A: Molecular and Biomolecular Spectroscopy*, 2010, 77, 175-178.

42 F. Wurm, A. M. Hofmann, A. Thomas, C. Dingels and H. Frey, *Macromol. Chem. Phys*., 2010, 211, 932-939.

43 K. Saint-Aubin, P. Poulin, H. Saadaoui, M. Maugey and C. Zakri, *Langmuir*, 2009, 25, 13206-13211.

44 N. H. Tran, A. S. Milev, M. A. Wilson, J. R. Bartlett and G. S. K. Kannangara, *Surf. Interface Anal.,* 2008, 40, 1294-1298.

45 J. U. Lee, J. Huh, K. H. Kim, C. Park and W. H. Jo, *Carbon,* 2007, 45, 1051-1057.

46 Y. Wang, L. Gao, J. Sun, Y. Liu, S. Zheng, H. Kajiura, Y. Li and K. Noda, *Chemical Physics*

Letters, 2006, 432, 205-208.

47 X. Mao, G. C. Rutledge and T. A. Hatton, *Langmuir*, 2013, 29, 9626-9634.

48 G. Díaz Costanzo, S. Ledesma, I. Mondragon and S. Goyanes, *J. Phys. Chem. C,* 2010, 114, 14347-14352.

49 M. F. Islam, E. Rojas, D. M. Bergey, A. T. Johnson and A. G. Yodh, *Nano Lett*., 2003, 3, 269-273.

50 D. K. Singh, P. K. Iyer and P. K. Giri, *Carbon*, 2012, 50, 4495-4505.

51 Y. Liu, J. Huang, M. Sun, J. Yu, Y. Chen, Y. Zhang, S. Jiang and Q. Shen, *Nanoscale*, 2014, 6, 1480-1489.

52 L. Zhao, D. A. Loy and K. J. Shea, *J. Am. Chem. Soc*., 2006, 128, 14250-14251.

53 J. Jiang, B. Qi, M. Lepage and Y. Zhao, *Macromolecules*, 2007, 40, 790-792.

54 J. Liu, J. Luo, R. Liu, J. Jiang and X. Liu, *Colloid Polym Sci*., 2014, 292, 153-161.

55 C. Park, S. Lee, J. H. Lee, J. Lim, S. C. Lee, M. Park, S. S. Lee, J. Kim, C. R. Park and C. Kim, *Carbon,* 2007, 45, 2072-2078.

56 M. Ates and N. Uludag, *Fibers and Polymers*, 2010, 11, 331-337.

57 X. Chen, Y. Wang, J. Zhou, W. Yan, X. Li and J. Zhu, *Anal. Chem*., 2008, 80, 2133-2140.

58 H. Gu, X. D. Su and K. P. Loh, *J. Phys. Chem. B*, 2005, 109, 13611-13618.

59 X. Pang, P. Imin, I. Zhitomirsky and A, Adronov, *Mcaromolecules*, 2010, 43, 10376-10381.

60 D. M. Guldi, G. M. Rahman, F. Zerbetto and M. Prato, *Acc. Chem. Res*., 2005, 38, 871-878.

61 E. Y. H. Teo, Q. D. Ling, Y. Song, Y. P. Tan, W. Wang, E. T. Kang, D. S. H. Chan and C. Zhu, *Organic Electronics*, 2006, 7, 173-180.

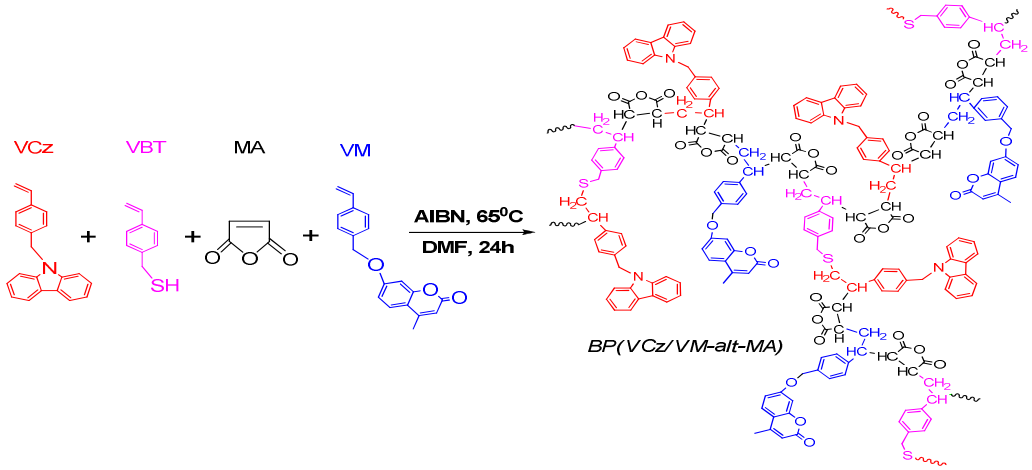

Scheme 1 The schematic illustration of synthesis of branched polymer BP(VCz/VM-*alt*-MA).

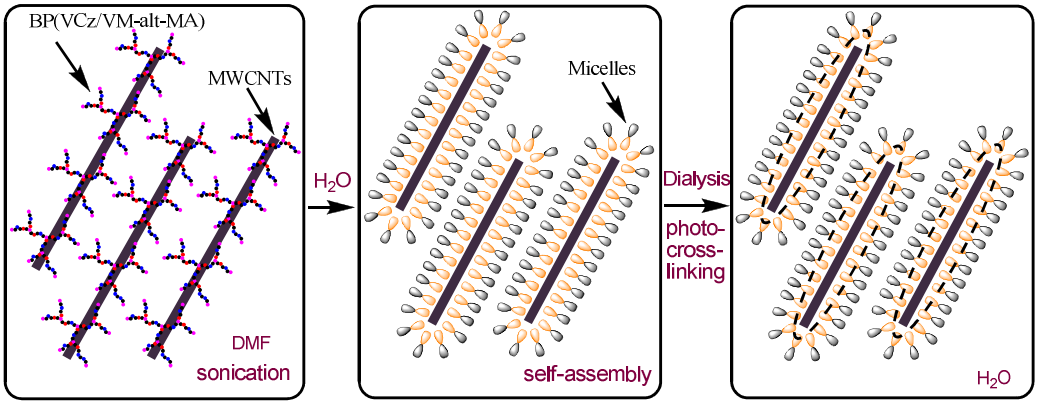

Scheme 2 Scheme for the formation of BPVCM micelle dispersing MWCNTs.

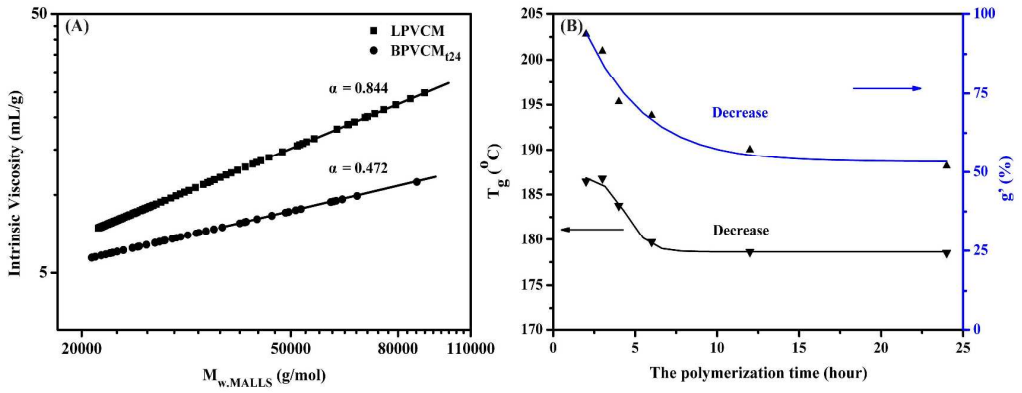

Fig. 1 (A) Mark-Houwink-Sakurada plot for branched polymer ($BPVCM_{t24}$) and linear polymer (LPVCM) and (B) Plots of the branching magnitude of g' (blue one) and the glass-transition temperature T_g (black one) on polymerization time.

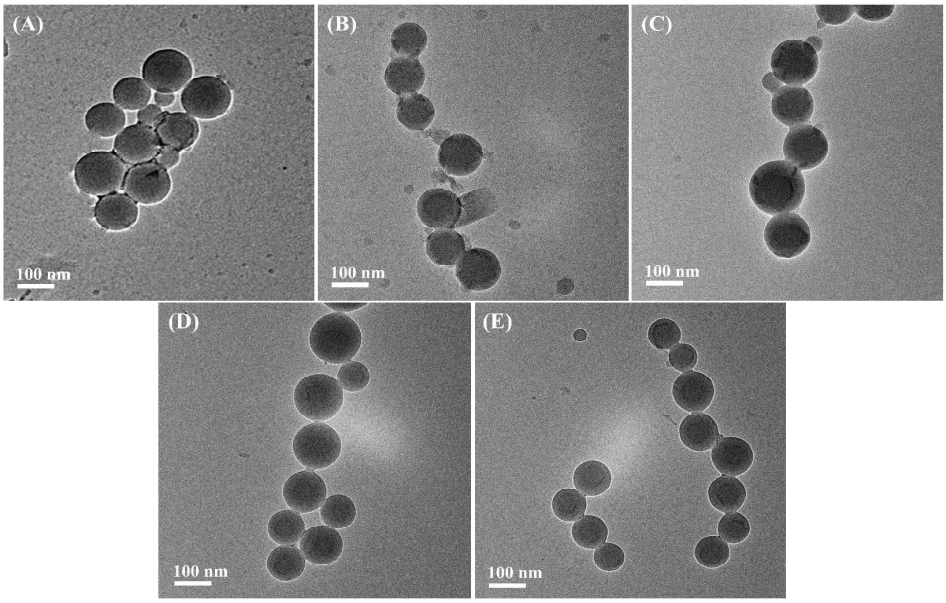

Fig. 2 TEM images of self-assemble micelles of copolymer. (A) LPVCM, (B) $BPVCM_{t24}$, (C) $BPVCM_4$, (D) $BPVCM_8$, (E) $BPVCM_{16,}$ The concentration of the micellar solution is 0.2 mg/mL.

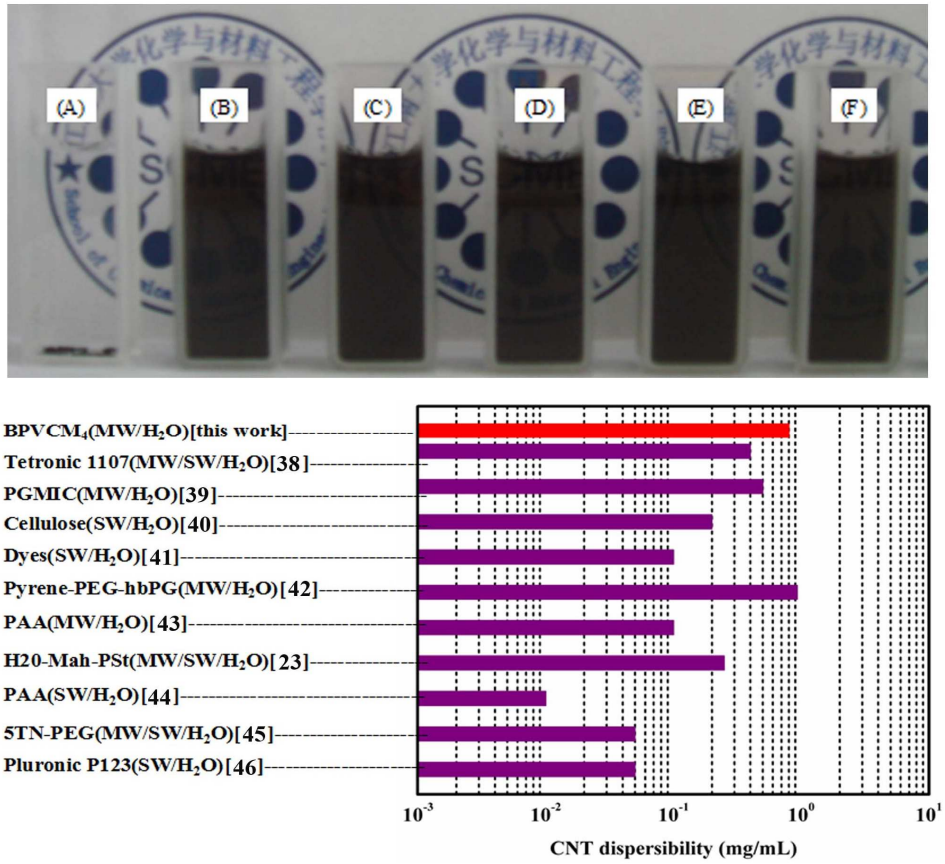

Fig. 3 Upper: Dispersions of a pristine MWCNTs (A) MWCNTs with polymers: (B) LPVCM, (C) $BPVCM_{t24}$, (D) $BPVCM_4$, (E) $BPVCM_8$, (F) $BPVCM_{16}$; The images were taken after 30 days of storage. The concentration of MWCNTs is 0.08 mg/mL, MWCNTs/copolymers = 1:2.5 (wt%). Down: Comparison of CNT dispersibility in aqueous solution using various non-covalent type dispersant.

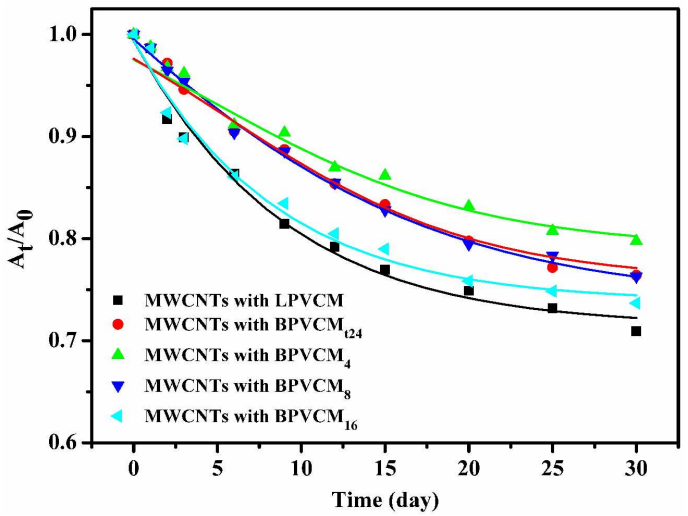

Fig. 4 UV-vis absorbance of MWCNTs functionalized by linear polymer LPVCM and branched copolymer BPVCM at the wavelength of 500 nm versus standing time. The concentration of the sample is 0.08 mg/mL.

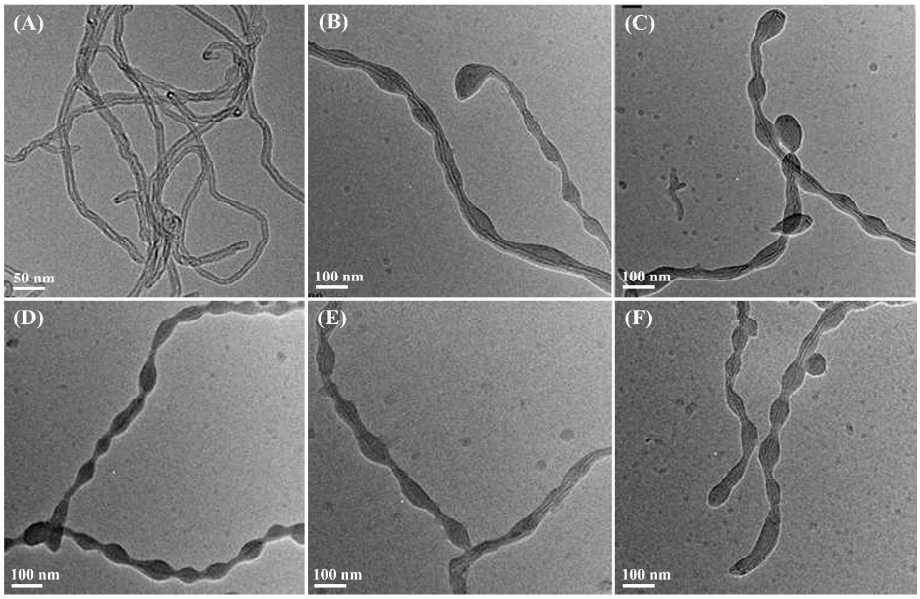

Fig. 5 TEM images of (A) pristine MWCNTs; MWCNTs functionalized with different polymer: (B) LPVCM, (C) $BPVCM_{t24}$, (D) $BPVCM_4$, (E) $BPVCM_8$, (F) $BPVCM_{16}$. The concentration of MWCNTs is 0.08 mg/mL, MWCNTs/copolymers = 1:2.5 (wt%).

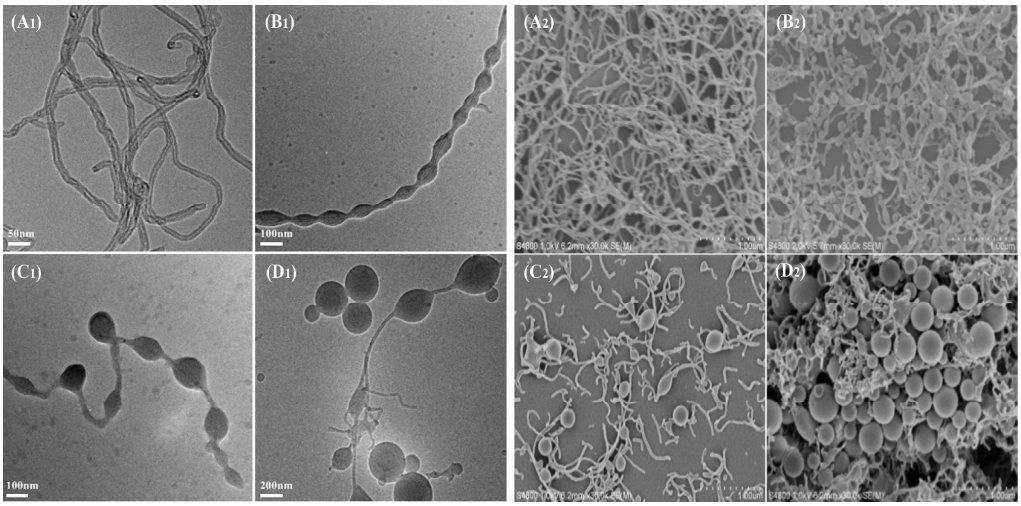

Fig. 6 TEM (Left) and SEM (Right) images of $BPVCM_4$ functionalized CNTs (the concentration of CNTs is 0.08 mg/mL): (A_1/A_2) pristine MWCNTs; (B_1/B_2) MWCNTs/$BPVCM_4$ = 1:2.5 (wt%); (C_1/C_2) MWCNTs/$BPVCM_4$ = 1:6.25 (wt%); (D_1/D_2) MWCNTs/$BPVCM_4$ = 1:12.5 (wt%).

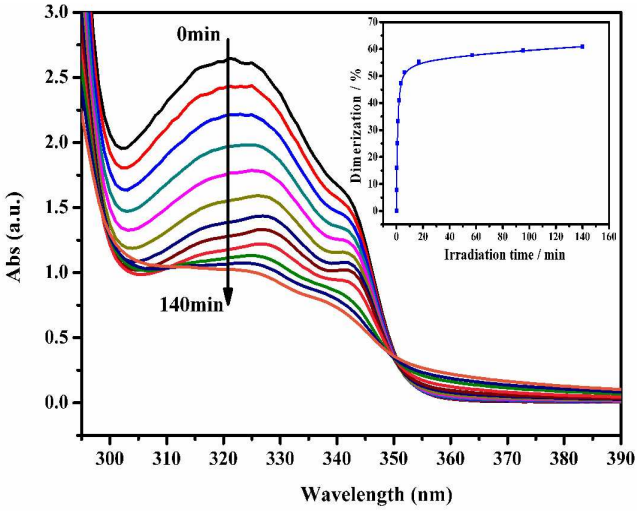

Fig. 7 UV-vis spectra of $BPVCM_4$ micelle with various irradiation times. Inset: The dimerization of $BPVCM_4$ micelle versus irradiation time. The concentration of micellar solution is 0.2 mg/mL, irradiation of UV light, $\lambda > 300$ nm.

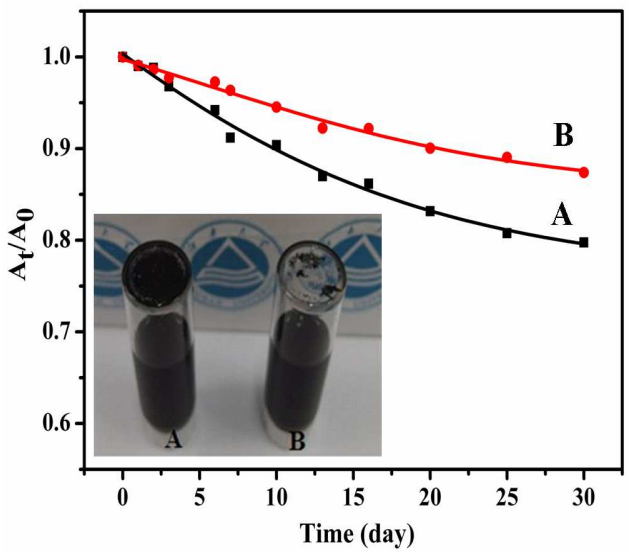

Fig. 8 UV-vis absorbance of BPVCM functionalized MWCNTs before (A) and after (B) irradiation with UV light at the wavelength of 500 nm versus standing time. Inset: The images were taken after 30 days storage. The concentration of the MWCNTs is 0.08 mg/mL, MWCNTs/$BPVCM_4$ = 1:2.5 (wt%).

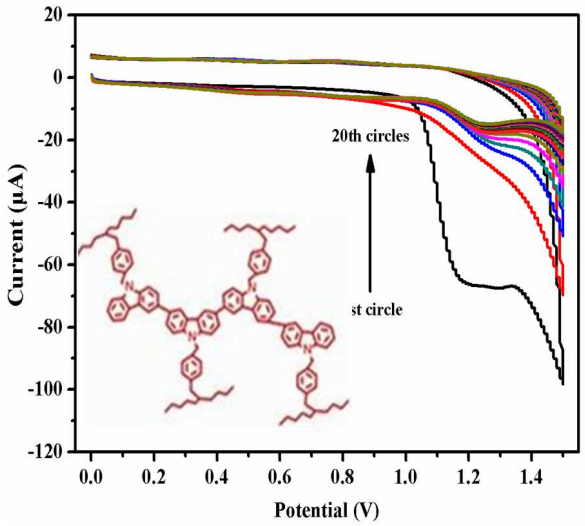

Fig. 9 The CV traces with BPVCM/MWCNTs modified GCE as the substrate with sweeping between 0-1.5 V. Scan rate of 100 mV/s in 0.1 M $LiClO_4$/ACN with a platinum wire as counter electrode and a saturated calomel electrode as reference electrode.

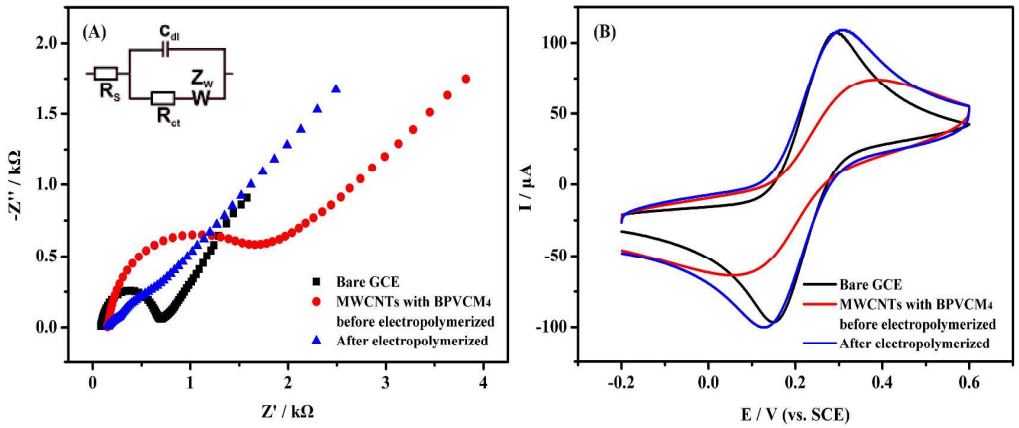

Fig. 10 Electrochemical impedance spectroscopy (EIS) (A) and CV (B) of BPVCM/MWCNTs before and after electropolymerization in 0.1 M KCl electrolyte solution containing 0.01 M $[Fe(CN)_6]^{3-/4-}$. Scan rate: 100 mV/s.